Underwater Sensing with Omni-Directional Stereo Camera

Atsushi Yamashita
Department of Precision Engineering
The University of Tokyo
7-3-1 Hongo, Bunkyo-ku,
Tokyo 113-8656, Japan
yamashita@ieee.org

Ryosuke Kawanishi Tadashi Koketsu Toru Kaneko
Department of Mechanical Engineering
Shizuoka University
3-5-1 Johoku, Naka-ku, Hamamatsu-shi,
Shizuoka 432–8561, Japan
tmtkane@ipc.shizuoka.ac.jp

Hajime Asama
Department of Precision Engineering
The University of Tokyo
7-3-1 Hongo, Bunkyo-ku,
Tokyo 113-8656, Japan
asama@robot.t.u-tokyo.ac.jp

Abstract

In this paper, we propose an underwater sensing method by using an omni-directional stereo camera system. When observing objects in water through a camera contained in a waterproof housing or observing objects in an aquarium tank filled with preserving liquid, we should solve a problem of light refraction at the boundary surfaces of refractive index discontinuity which gives image distortion. The proposed method uses two omni-directional cameras that have wide field of view to measure underwater environments. A ray tracing technique solves the problem of image distortion caused by refractive index discontinuity. Experimental results show the validity of the proposed method.

1. Introduction

In this paper, we propose an underwater sensing method by using an omni-directional stereo camera system.

In recent years, demands of underwater tasks have increased. For example, digging of ocean bottom resources, exploration of aquatic environments, rescues, and salvages become important. To execute these tasks instead of human, there are a lot of studies about underwater robots or underwater sensing systems for observing underwater situations correctly and robustly from cameras of these systems [1]. However, it is not easy to observe underwater environments with cameras [2–4], because of the following three big problems; (1) light attenuation effect, (2) light disturbing effect, and (3) light refraction effect.

The first problem is about the attenuation effects of light. The light intensity decreases with the distance from objects in water by light attenuation depending on the wavelength of light. For example, red light decreases easier than blue light in water [2]. As a result, underwater images become bluish, and colors of objects observed in underwater environments are different from those in air (Figure 1(a)).

The second problem is about view-disturbing noises, such as bubble noises, small fishes, small creatures, and so on. View-disturbing noises may disturb camera's field of view (Figure 1(b)).

It becomes very difficult under those two problems to detect or to recognize objects in water by observing their textures and colors.

As to the above-mentioned problems, methods or theories for aerial environments can be applicable for underwater sensing by considering the behavior of light in water. Several image processing techniques can be effective for removing adherent noises. Color information can be also restored by considering reflection, absorption, and scattering phenomena of light in theory [2]. Indeed, underwater sensing methods for the light attenuation problem [5] and for the view-disturbing noise problem [6] have already been proposed.

The third problem is about the light refraction effects. Several problems occur and a precise measurement cannot be achieved under the condition that cameras and objects are in the different condition where the refraction indices differ from each other.

A rectangular object in a jar filled with air and an ob-

(a) Light attenuation effect. (b) Light disturbing effect.

Figure 1. Problems of underwater sensing. (a) Underwater images become bluish, and colors of objects observed in underwater environments are different from those in air. (b) Bubble noises disturb camera's field of view.

(a) Object without water. (b) Object with water.

Figure 2. Problems of light refraction effect. (a) A rectangular object in a jar filled with air. (b) A rectangular object in a jar filled half with water.

ject in a jar filled half with water are shown in Figs. 2(a) and (b), respectively. Figures 2(a) and (b) look different, although they are same objects. Accurate results cannot be obtained from the measurement using the distorted image without considering the influence of light refraction. This problem occurs not only when the object in a container filled with liquid is observed by using the camera outside of liquid but also when the camera is put into liquid with waterproof housing. This is because the housing case for waterproof is filled with air and light refraction occurs at the boundary of air and water.

As to the light refraction problem, three-dimensional (3-D) measurement methods in aquatic environments are also proposed [7–10]. However, techniques that do not consider the influence of the refraction effects [7–9] may have the problems of accuracy.

Accurate 3-D measurement methods of objects in liquid [11–14] with a laser range finder and by using a space encoding method [15] by considering the refraction effects are also proposed. However, it is difficult to measure moving objects with a laser range finder or a space encoding method.

A stereo camera system is suitable for measuring moving objects, though the methods by using a stereo camera system [10] have the problem that the corresponding points are difficult to detect when the texture of the object's surface is simple in particular when there is the refraction on the boundary between the air and the liquid. The method by the use of motion stereo images obtained with a moving camera [16] also has the problem that the relationship between the camera and the object is difficult to estimate because the camera moves. The surface shape reconstruction method of objects by using an optical flow [17] is not suitable for the accurate measurement, too.

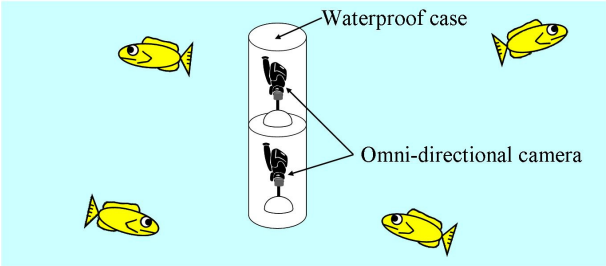

Figure 3. Underwater sensing by using an omni-directional stereo camera system.

By using properly calibrated stereo systems, underwater measurements of moving objects can be achieved [6,18,19]. However, it is not easy to continue to track and measure the same moving objects. This is because a conventional camera has a limited field of view and the common field of view of two conventional cameras is not wide. To solve this problem, an omni-directional camera which has a wide field of view has been invented [20]. Taking account of installation on robots, an omni-directional camera is suitable because it can get a surrounding view image at once. It is shown that an omni-directional camera is effective in measurement and recognition in environment [21–23].

There are few studies about a stereo vision method using two omni-directional cameras in water, while there are a lot of studies in aerial environments such as [24–26]. In this paper, we propose an underwater sensing method by using an omni-directional stereo camera system (Figure 3).

The composition of this paper is detailed below. Section 2 describes the outline of the proposed method and a 3-D measurement method that are based on the ray tracing technique. Section 3 mentions about experiments and discussions about underwater sensing. Section 4 describes conclusions and future works.

2. 3-D Measurement Method

2.1. Overview

Stereo image pairs are acquired by using two omni-directional cameras.

The omni-directional camera we use has a hyperboloid

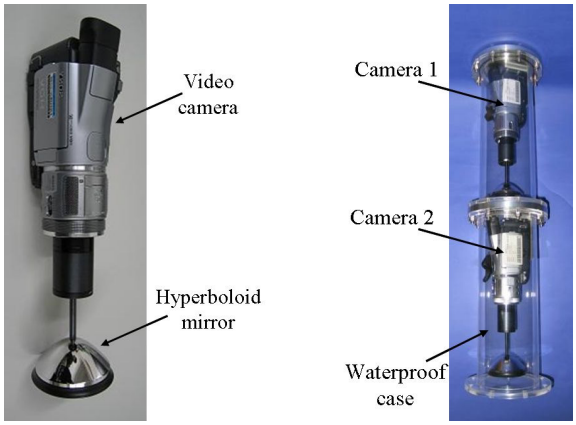

(a) Omni-directional camera. (b) Stereo camera.

Figure 4. Omni-directional stereo camera system with waterproof case. Two omni-directional cameras are arranged in tandem.

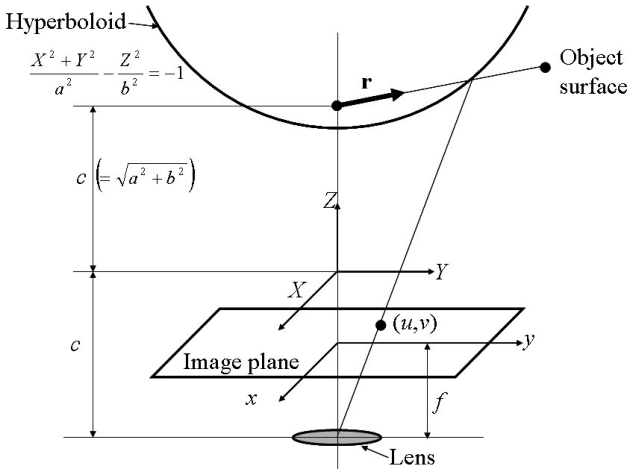

Figure 5. Relationship of lens, image plane, and hyperboloid mirror. Ray vector **r** is directed from the focus of the hyperboloid mirror to the refection point of the ray on the mirror surface.

mirror in front of a lens of a conventional camera [27] (Figure 4(a)). For use in mobile robot, two omni-directional cameras are sometimes arranged abreast such as [24]. In this case, one camera disturbs the field of view of another camera, and measurable region of the stereo camera becomes narrow. Therefore, two omni-directional cameras are arranged in tandem such as [26] (Figure 4(b)). Two cameras are covered with an acrylic waterproof case.

All intrinsic and extrinsic parameters of two cameras are calibrated in advance. The relationship between two cameras and the boundary of the refraction is also calibrated in advance of the measurement.

In measurement, corresponding points are searched for in acquired stereo image pairs at first. Two rays are calculated by ray tracing from the left and the right images by using Snell's law of refraction. The intersection of the two rays gives the 3-D coordinates of the target point in water.

2.2. Ray Vector from Camera

Ray vectors from the omni-directional cameras can be calculated by using camera parameters.

We define a unit vector originating from the center of projection to an object point in 3-D space as a ray vector $r = (x, y, z)^{\mathrm{T}}$, where T stands for transposition of vector or matrix. As shown in Figure 5, ray vector **r** is directed from the focus of the hyperboloid mirror to the refection point of the ray on the mirror surface.

Ray vector **r** is calculated from image coordinates $(u, v)^{\mathrm{T}}$ of the feature using (1) and (2).

$$\mathbf{r} = \frac{1}{(su)^2+(sv)^2+(sf-2c)^2}\begin{pmatrix} su \\ sv \\ sf-2c \end{pmatrix}, \quad (1)$$

$$s = \frac{a^2(f\sqrt{a^2+b^2}+b\sqrt{u^2+v^2+f^2})}{a^2f^2-b^2(u^2+v^2)}. \quad (2)$$

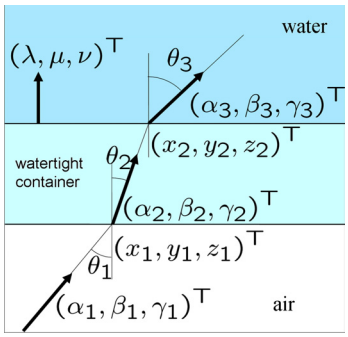

Figure 6. Light refraction effect from air to water. Ray tracing can be done by considering Snell's law of refraction.

where a, b and c $(= \sqrt{a^2+b^2})$ are the hyperboloid parameters, and f is the image distance (the distance between the image plane and the center of projection, or the center of the lens) of camera, respectively.

2.3. Optical Ray Tracing

The ray from the left image is refracted at the boundary of air and waterproof container, and then is refracted at the boundary of waterproof container and water. Finally, the ray projects onto the object in water, and then the ray reflected by the object is refracted again at the boundary of water, container, and air to project onto the right image plane of the camera. This phenomenon can be analyzed by ray tracing [10].

Figure 6 shows light refraction effects from air to watertight container and from watertight container to water.

Here, let refractive indices of air and waterproof case be n_1 and n_2, incident and refractive angles from air to waterproof case be θ_1 and θ_2, respectively. A unit vector of ray

in waterproof case $(\alpha_2, \beta_2, \gamma_2)^{\mathrm{T}}$ can be calculated by using a unit vector of ray from air $(\alpha_1, \beta_1, \gamma_1)^{\mathrm{T}}$ and a unit normal vector of waterproof case $(\lambda_1, \mu_1, \nu_1)^{\mathrm{T}}$ as follows.

$$\begin{pmatrix} \alpha_2 \\ \beta_2 \\ \gamma_2 \end{pmatrix} = \frac{n_1}{n_2} \begin{pmatrix} \alpha_1 \\ \beta_1 \\ \gamma_1 \end{pmatrix} + c_1, \tag{3}$$

where

$$c_1 = \left\{ \sqrt{1 - \left(\frac{n_1}{n_2}\right)^2 \sin^2\theta_1} - \frac{n_1}{n_2}\cos\theta_1 \right\} \begin{pmatrix} \lambda \\ \mu \\ \nu \end{pmatrix}.$$

A unit vector in water $(\alpha_3, \beta_3, \gamma_3)^{\mathrm{T}}$ is also calculated by using the refractive index of water n_3 and the refractive angle of water θ_3.

$$\begin{pmatrix} \alpha_3 \\ \beta_3 \\ \gamma_3 \end{pmatrix} = \frac{n_2}{n_3} \begin{pmatrix} \alpha_2 \\ \beta_2 \\ \gamma_2 \end{pmatrix} + c_2, \tag{4}$$

where

$$c_2 = \left\{ \sqrt{1 - \left(\frac{n_2}{n_3}\right)^2 \sin^2\theta_2} - \frac{n_2}{n_3}\cos\theta_2 \right\} \begin{pmatrix} \lambda \\ \mu \\ \nu \end{pmatrix}.$$

When Snell's law of refraction is applied, the following equation is obtained:

$$\theta_2 = \sin^{-1}\left(\frac{n_1}{n_2}\sin\theta_1\right). \tag{5}$$

The ray from the camera finally reaches on the surface of the underwater object at the point P $(x_P, y_P, z_P)^{\mathrm{T}}$.

$$\begin{pmatrix} x_P \\ y_P \\ z_P \end{pmatrix} = k \begin{pmatrix} \alpha_3 \\ \beta_3 \\ \gamma_3 \end{pmatrix} + \begin{pmatrix} x_2 \\ y_2 \\ z_2 \end{pmatrix}, \tag{6}$$

where k is a constant and $(x_2, y_2, z_2)^{\mathrm{T}}$ is the intersection point between the ray from waterproof case and the refraction boundary, respectively.

2.4. Corresponding Point

The relationship between corresponding points of the left and the right images is formulated with epipolar constraints, and the corresponding points exist on the epipolar lines. In aerial environments, the epipolor line is usually straight [1]. However, the epipolar lines are not always straight in aquatic environments because of the refraction of light. Therefore, we calculate the epipolar lines with the ray tracing technique in the same way of Section 2.3.

[1]Strictly speaking, the epipolar line is not always straight in aerial environments. It depends on the configuration of the stereo rig.

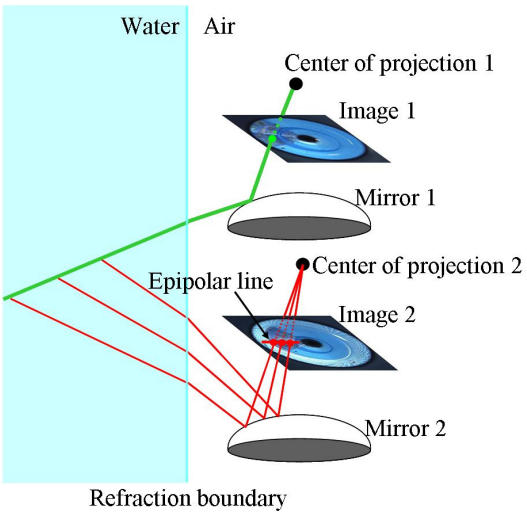

Figure 7. Epipolar line of underwater stereo measurement. Epipolar line is not always straight in water.

The calculation method of epipolar lines is as follows. Ray tracing is executed from an image of the camera 1 (Figure 7). In other words, the ray is searched from the lens center of the camera 1. The ray from the camera 1 finally reaches in water and the ray is expressed as line in a 3-D coordinates (Green line in Figure 7).

Then, the ray from camera 1 is projected onto image 2. From each point of the ray from camera 1, the ray tracing to the lens center of the camera 2 is executed by considering the effect of light refraction on the refractive boundary and that of light reflection on the mirror of the omni-directional camera. Each ray from the mirror to lens center intersects with image plane 2, and epipolar line consists of these intersection points (Red line in Figure 7).

After obtaining epipolar lines, corresponding points on epipolar lines are searched for with template matching by using the normalized cross correlation (NCC) method. Original omni-directional images have distortions and the accuracy of the template matching is not high by using omni-directional images. Therefore, omni-directional images are converted to panoramic images, and epipolar lines are also converted onto the panoramic images (Figure 8). Note that the epipolar line in Figure 8 looks straight, however, it is not straight in a precise sense. Generally speaking, epipolar lines in stereo measurement in water are curved, and we must consider shapes of epipolar lines exactly in water to detect corresponding points precisely.

2.5. 3-D Measurement

Two rays are calculated by ray tracing from the left and the right images, and the intersection of the two rays gives the 3-D coordinates of the target point in water.

After corresponding point and disparity of each pixel are

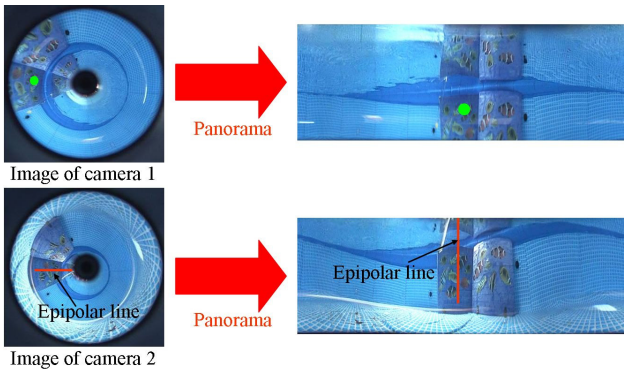

Figure 8. Panorama images. Omni-directional images are converted to panoramic images, and epipolar lines are also converted onto the panoramic images.

acquired, the 3-D position of each corresponding point can be measured with triangulation.

3. Experiment

3.1. Experimental Setup

The omni-directional camera we used in the experiment is a combination of an HDV camera (Sony HDR-HC1) and a hyperboloid mirror (Suekage SOIOS70-scope). An image sequence was acquired with the image size of 1920×1080 pixel and the image capture rate was 30fps. The stereo camera system was covered with an acrylic waterproof case whose refractive index is 1.49.

Camera calibration was executed by capturing images of the planner pattern on which surface checked patterns were drawn. Intrinsic parameters of each camera (image distance f, optical center, distortion parameters [28], and so on), parameters of two hyperboloid mirrors (a and b), the relationship between cameras (5DOF, rotation along optical axis was not calibrated because it is not necessary for omni-directional cameras), the relationship between the stereo cameras and the waterproof case (5DOF) were calibrated. The baseline length (the distance between two cameras) was calibrated as 376mm.

3.2. Evaluation of Accuracy

Figure 9 shows the measured object that consists of two planes. In the planes, fishes were drawn. The objects and the stereo camera system were inside the pool filled with water whose refractive index is 1.33.

Figure 10 shows the overview of the experimental setup. The distance between the stereo camera system and the object was about 900mm.

Figure 11 shows the example of the acquired image pairs. The target object was on the lower side of images.

Figure 12 shows the 3-D measurement result of the object. In Figure 12(a), the plane 1 is drawn by red color and the plane 2 is drawn by blue color, respectively. The backgrounds (blue color regions in Figure 9) were not measured because corresponding points were not detected in these regions that had no textures. On the other hands, the shapes of fishes can be recognized because they had rich textures. Figure 12(b) shows the 3-D measurement result by birds-eye view.

Figure 9. Object that consists of two planes. Pictures of fishes are drawn on the object.

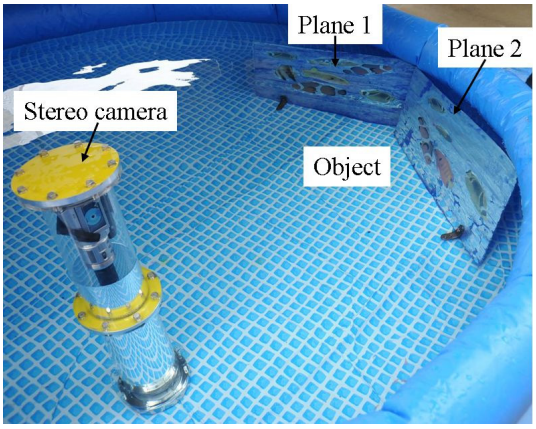

Figure 10. Overview of experiment. The omni-directional stereo camera system and the object are inside pool filled with water.

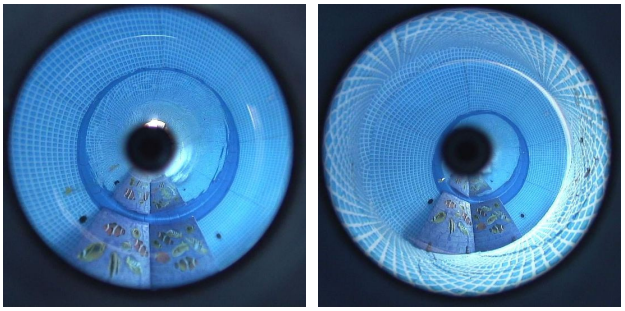

(a) Image of camera 1. (b) Image of camera 2.

Figure 11. Examples of aquatic images. The target object was on the lower side of images.

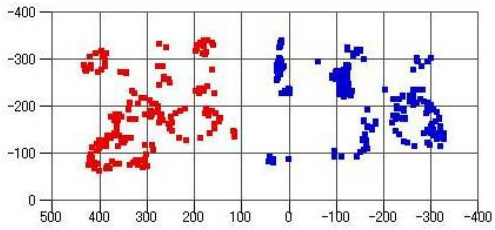

(a) Frontal view.

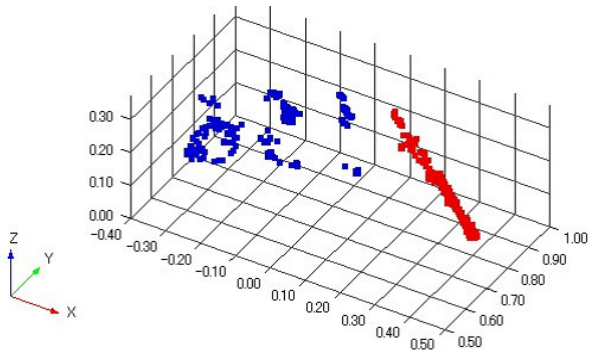

(b) Birds-eye view.

Figure 12. 3-D measurement result of two planes. The plane 1 is drawn by red color and the plane 2 is drawn by blue color, respectively.

Table 1. Standard deviation.

	Standard deviation
Plane 1	13.4mm
Plane 2	9.0mm

To evaluate the measurement result of Figure 12 quantitatively, shape reconstruction error is measured. Least square planes of the plane 1 and plane 2 are constructed. Table 1 shows the standard deviation of measurement points on each plane from each least square plane. Standard deviation is within 15mm while the object distance is about 900mm.

To evaluate the validity of considering the light refraction effects, the accuracy of the shape reconstruction is compared between with consideration of the refraction effects and without considering it.

Another object whose size was known (Figure 13) was measured with consideration of refractive effects and without considering it, respectively. Table 2 shows the measurement results of distances a, b, c, and d with and without consideration of the light refraction effects, respectively. Maximum error without considering the light refraction effects is 88.5%, while that with considering it is 14.1%. Variation of error is very large without considering the light refraction effects (28.1%–88.5%). Error of longitudinal direction is larger than that of transverse direction. Therefore, error

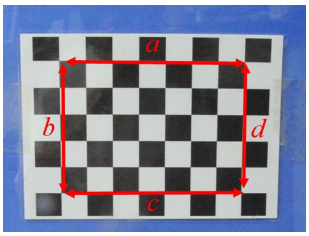

Figure 13. Object whose size is known. $a = c = 210mm$. $b = d = 150mm$.

Table 2. Effects of ray tracing. (1) Ground truth. (2) Result without consideration of the light refraction effects. Upper column: measurement result. Lower column: error. (3) Result with consideration of the light refraction effects.

	a	b	c	d
(1)	210.0mm	150.0mm	210.0mm	150.0mm
(2)	270.0mm	283.0mm	269.1mm	282.8mm
	(28.5%)	(88.0%)	(28.1%)	(88.5%)
(3)	192.0mm	140.6mm	180.4mm	137.4mm
	(8.6%)	(6.3%)	(14.1%)	(8.4%)

tendency exists. On the other hands, error tendency is small (6.3%–14.1%) when considering it.

From these results, the effectiveness of considering the light refraction effects and was verified.

3.3. Evaluation of Field of View

To evaluate the wide field of view of the camera, a moving object was measured. The object was moving around the stereo camera system. The measurement result is shown in Figure 14. Blue dots indicate the focal points of mirrors and red dots mean the target positions, respectively.

From this result, it is verified that moving targets can be measured continuously and stably thanks to the wide field of view of the proposed stereo camera system.

4. Conclusion

In this paper, we propose an underwater sensing method by using an omni-directional stereo camera system. We solve a problem of light refraction at the boundary surfaces of refractive index discontinuity which gives image distortion. The proposed method uses two omni-directional cameras that have wide field of view to measure underwater environments. Experimental results show the validity of the proposed method.

As a future work, the proposed omni-directional stereo camera system should be attached to a underwater robot to measure underwater environments automatically. It is very important to improve the measurement accuracy by developing the assembly accuracy of the camera system and ac-

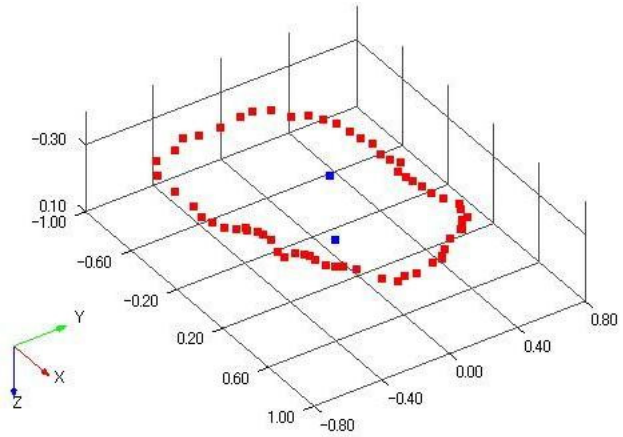

Figure 14. 3-D measurement result of the moving object. Blue dots indicate the focal points of mirrors and red dots mean the target positions, respectively.

curacy of the calibration [29], and to formulate the epipolar constraints more technically [30, 31].

Acknowledgements

This work was in part supported by The Ministry of Education, Culture, Sports, Science and Technology (MEXT) KAKENHI, Grant-in-Aid for Young Scientist (A), 22680017.

References

[1] Junku Yuh and Michael West: "Underwater Robotics," *Advanced Robotics*, Vol.15, No.5, pp.609–639, 2001.

[2] E. O. Hulburt: "Optics of Distilled and Natural Water," *Journal of the Optical Society of America*, Vol.35, pp.689–705, 1945.

[3] W. Kenneth Stewart: "Remote-Sensing Issues for Intelligent Underwater Systems," *Proceedings of the 1991 IEEE Computer Society Conference on Computer Vision and Pattern Recognition* (*CVPR1991*), pp.230–235, 1991.

[4] Frank M. Caimi: *Selected Papers on Underwater Optics*, *SIPE Milestone Series*, Vol.MS118, 1996.

[5] Atsushi Yamashita, Megumi Fujii and Toru Kaneko: "Color Registration of Underwater Images for Underwater Sensing with Consideration of Light Attenuation," *Proceedings of the 2007 IEEE International Conference on Robotics and Automation* (*ICRA2007*), pp.4570–4575, 2007.

[6] Atsushi Yamashita, Susumu Kato and Toru Kaneko: "Robust Sensing against Bubble Noises in Aquatic Environments with a Stereo Vision System," *Proceedings of the 2006 IEEE International Conference on Robotics and Automation* (*ICRA2006*), pp.928–933, 2006.

[7] Bryan W. Coles: "Recent Developments in Underwater Laser Scanning Systems," *SPIE Vol.980 Underwater Imaging*, pp.42–52, 1988.

[8] Robert F. Tusting and Daniel L. Davis: "Laser Systems and Structured Illumination for Quantitative Undersea Imaging," *Marine Technology Society Journal*, Vol.26, No.4, pp.5–12, 1992.

[9] Nathalie Pessel, Jan Opderbecke, Marie-Jose Aldon: "Camera Self-Calibration in Underwater Environment," *Proceedings of the 11th International Conference in Central Europe on Computer Graphics, Visualization and Computer Vision*, (*WSCG2003*), pp.104–110, 2003.

[10] Rongxing Li, Haihao Li, Weihong Zou, Robert G. Smith and Terry A. Curran: "Quantitive Photogrammetric Analysis of Digital Underwater Video Imagery," *IEEE Journal of Oceanic Engineering*, Vol.22, No.2, pp.364–375, 1997.

[11] Atsushi Yamashita, Etsukazu Hayashimoto, Toru Kaneko and Yoshimasa Kawata: "3-D Measurement of Objects in a Cylindrical Glass Water Tank with a Laser Range Finder," *Proceedings of the 2003 IEEE/RSJ International Conference on Intelligent Robots and Systems* (*IROS2003*), pp.1578–1583, 2003.

[12] Atsushi Yamashita, Hirokazu Higuchi, Toru Kaneko and Yoshimasa Kawata: "Three Dimensional Measurement of Object's Surface in Water Using the Light Stripe Projection Method," *Proceedings of the 2004 IEEE International Conference on Robotics and Automation* (*ICRA2004*), pp.2736–2741, 2004.

[13] Hayato Kondo, Toshihiro Maki, Tamaki Ura, Yoshiaki Nose, Takashi Sakamaki and Masaaki Inaishi: "Relative Navigation of an Autonomous Underwater Vehicle Using a Light-Section Profiling System," *Proceedings of the 2004 IEEE/RSJ International Conference on Intelligent Robots and Systems* (*IROS2004*), pp.1103–1108, 2004.

[14] Atsushi Yamashita, Shinsuke Ikeda and Toru Kaneko: "3-D Measurement of Objects in Unknown Aquatic Environments with a Laser Range Finder," *Proceedings of the 2005 IEEE International Conference on Robotics and Automation* (*ICRA2005*), pp.3923–3928, 2005.

[15] Ryohei Kawai, Atsushi Yamashita and Toru Kaneko: "Three-Dimensional Measurement of Objects in Water by Using Space Encoding Method," *Proceedings of the 2009 IEEE International Conference on Robotics and Automation* (*ICRA2009*), pp.2830–2835, 2009.

[16] Hideo Saito, Hirofumi Kawamura and Msasato Nakajima: "3D Shape Measurement of Underwater Objects Using Motion Stereo," *Proceedings of 21th International Conference on Industrial Electronics, Control, and Instrumentation*, pp.1231–1235, 1995.

[17] Hiroshi Murase: "Surface Shape Reconstruction of a Nonrigid Transparent Object Using Refraction and Motion," *IEEE Transactions on Pattern Analysis and Machine Intelligence*, Vol.14, No.10, pp.1045–1052, 1992.

[18] Atsushi Yamashita, Akira Fujii and Toru Kaneko: "Three Dimensional Measurement of Objects in Liquid and Estimation of Refractive Index of Liquid by Using Images of Water Surface with a Stereo Vision System," *Proceedings of the 2008 IEEE International Conference on Robotics and Automation* (*ICRA2008*), pp.974–979, 2008.

[19] Atsushi Yamashita, Yudai Shirane and Toru Kaneko: "Monocular Underwater Stereo –3D Measurement Using Difference of Appearance Depending on Optical Paths–," *Proceedings of the 2010 IEEE/RSJ International Conference on Intelligent Robots and Systems* (*IROS2010*), pp.3652–3657, 2010.

[20] Shree K. Nayar: "Catadioptric Omnidirectional Camera," *Proceedings of the 1997 IEEE Computer Society Conference on Computer Vision and Pattern Recognition* (*CVPR1997*), pp.482–488, 1997.

[21] Joshua Gluckman and Shree K. Nayar: "Ego-Motion and Omnidirectional Cameras," *Proceedings of the 6th IEEE International Conference on Computer Vision (ICCV1998)*, pp.999–1005, 1998.

[22] Ryosuke Kawanishi, Atsushi Yamashita and Toru Kaneko: "Estimation of Camera Motion with Feature Flow Model for 3D Environment Modeling by Using Omni-Directional Camera," *Proceedings of the 2009 IEEE/RSJ International Conference on Intelligent Robots and Systems* (*IROS2009*), pp.3089–3094, 2009.

[23] Kenki Matsui, Atsushi Yamashita and Toru Kaneko: "3-D Shape Measurement of Pipe by Range Finder Constructed with Omni-Directional Laser and Omni-Directional Camera," *Proceedings of the 2010 IEEE International Conference on Robotics and Automation* (*ICRA2010*), pp.2537–2542, 2010.

[24] Hiroshi Ishiguro, Masashi Yamamoto and Saburo Tsuji: "Omni-Directional Stereo," *IEEE Transactions on Pattern Analysis and Machine Intelligence*, Vol.14, No.2, pp.257–262, 1992.

[25] Jun-ichi Takiguchi, Minoru Yoshida, Akito Takeya, Jyunichi Eino and Takumi Hashizume: "High Precision Range Estimation from an Omnidirectional Stereo System," *Proceedings of the 2002 IEEE/RSJ International Conference on Intelligent Robots and Systems* (*IROS2002*), pp.263–268, 2002.

[26] Hiroshi Koyasu, Jun Miura and Yoshiaki Shirai: "Recognizing Moving Obstacles for Robot Navigation Using Real-time Omnidirectional Stereo Vision," *Journal of Robotics and Mechatronics*, Vol.14, No.2, pp.147–156, 2002.

[27] Kazumasa Yamazawa, Yasushi Yagi and Masahiko Yachida: "Omnidirectional Image Sensor –HyperOmni Vision–," *Proceedings of the 3rd International Conference on Automation Technology*, Vol.5, pp.125–132, 1994.

[28] Juyang Weng, Paul Cohen and Marc Herniou: "Camera Calibration with Distortion Models and Accuracy Evaluation," *IEEE Transactions on Pattern Analysis and Machine Intelligence*, Vol.14, No.10, pp.965–980, 1992.

[29] Branislav Micusik and Tomas Pajdla: "Autocalibration & 3D Reconstruction with Non-Central Catadioptric Cameras," *Proceedings of the 2004 IEEE Computer Society Conference on Computer Vision and Pattern Recognition* (*CVPR2004*), Vol.1, pp.58–65, 2004.

[30] Yuanyuan Ding, Jingyi Yu and Peter Sturm: "Multi-perspective Stereo Matching and Volumetric Reconstruction," *Proceedings of the 12th IEEE International Conference on Computer Vision (ICCV2009)*, pp.1827–1834, 2009.

[31] Yuichi Taguchi, Amit Agrawal, Ashok Veeraraghavan, Srikumar Ramalingam and Ramesh Raskar: "Axial-Cones: Modeling Spherical Catadioptric Cameras for Wide-Angle Light Field Rendering," *ACM Transactions on Graphics* (*Proceedings of SIGGRAPH Asia 2010*), Vol.29, No.6, pp.172:1–172:8, 2010.